

Tissue-Engineered Myocardial Patch Derived From Extracellular Matrix Provides Regional Mechanical Function

Paul V. Kochupura, MD; Evren U. Azeloglu, MS; Damon J. Kelly, MS; Sergey V. Doronin, PhD; Stephen F. Badylak, MD, PhD, DVM; Irvin B. Krukenkamp, MD; Ira S. Cohen, MD, PhD; Glenn R. Gaudette, PhD

Background—Extracellular matrix (ECM), a tissue-engineered scaffold, recently demonstrated cardiomyocyte population after myocardial implantation. Surgical restoration of myocardium frequently uses Dacron as a myocardial patch. We hypothesized that an ECM-derived myocardial patch would provide a mechanical benefit not seen with Dacron.

Methods and Results—Using a canine model, a full thickness defect in the right ventricle was repaired with either Dacron or ECM. A third group had no surgery and determined baseline RV function. Eight weeks later, global systolic function was assessed by the preload recruitable stroke work relationship. Regional systolic function was measured by systolic area contraction (SAC), calculated by high density mechanical mapping. Tau was used to assess global diastolic function. Recoil rate and diastolic shear were used as measures of regional diastolic function. After functional data acquisition, tissue was fixed for histological evaluation. Global systolic and diastolic functions were similar at baseline and after ECM and Dacron implantation. Regional systolic function was greater in the ECM group compared with the Dacron group (SAC: $4.1 \pm 0.9\%$ versus -1.8 ± 1.1 , $P < 0.05$). Regional diastolic function was also greater in the ECM group (recoil rate ($^{\circ} \text{sec}^{-1}$): -44 ± 7 versus -17 ± 2 , ECM versus Dacron; $P < 0.05$). Immunohistochemical analysis revealed cardiomyocytes in the ECM implant region, a finding not seen with Dacron.

Conclusion—At 8 weeks, an ECM-derived tissue-engineered myocardial patch provides regional mechanical function, likely related to cardiomyocyte population. These results are in sharp contrast to Dacron, a commonly used myocardial patch. (*Circulation*. 2005;112[suppl I]:I-144–I-149.)

Key Words: heart failure ■ surgery ■ mechanics ■ remodeling ■ myocytes

Heart failure is a notoriously progressive disease, despite medical management.¹ The increasing gap between the incidence of end-stage heart failure and surgical treatment is due, in great part, to the shortage of donor organs.² In 2002, only 2154 heart transplants were performed, despite an annual average of 50 000 deaths related to New York Heart Association stage IV congestive heart failure.³ In addition to transplantation, other surgical modalities may play an increasingly important role in treatment of end-stage heart failure. These include ventricular assist devices, surgical restoration, passive constraint devices, coronary artery bypass grafting, and mitral valve repair.⁴

Another surgical approach to heart failure underscores the importance of the geometry of the ventricle. In most cases of heart failure, the ventricle assumes a dilated, spherical shape, decreasing the efficiency of ventricular contraction. In this instance, revascularization alone would not be sufficient to improve systolic function. This alternate approach is based on

the premise of restoring the normal ellipsoidal shape of the left ventricle from its decompensated, globular form.^{5–9} This principle was illustrated in the Surgical Anterior Ventricular Endocardial Restoration trial, which combined surgical restoration of an akinetic or dyskinetic anterior wall with Dacron and concomitant coronary artery bypass grafting or mitral valve repair.¹⁰ This strategy demonstrated an immediate improvement in ejection fraction, with sustained benefit and minimal morbidity.¹⁰

Tissue engineering offers possibilities beyond Dacron.¹¹ Specifically, it seeks to create organic scaffolds that both restore the geometry of the ventricle and attract or house cellular elements better suited for myocardial function.^{12–14} Thus, the development of a tissue-engineered myocardial patch (TEMP) represents the next frontier in the evolving surgical treatment of heart failure. Recently, Badylak et al¹⁵ investigated the use of porcine urinary bladder extracellular matrix (ECM), a biologically latent membrane

From the Departments of Surgery (P.V.K., I.B.K., G.R.G.) and Biomedical Engineering (E.U.A., D.J.K., I.B.K., G.R.G.), Stony Brook University, Stony Brook, New York; the McGowan Institute for Regenerative Medicine (S.F.B.), Pittsburgh, Pa; the Institute of Molecular Cardiology (S.V.D., I.B.K., I.S.C., G.R.G.), Stony Brook, New York; and the Department of Surgery (G.R.G.), University of Massachusetts Medical School, Worcester, Mass.

Correspondence to Glenn R. Gaudette, PhD, Department of Surgery, University of Massachusetts Medical School, 55 Lake Ave North, Worcester, MA 01655. E-mail glenn.gaudette@umassmed.edu

© 2005 American Heart Association, Inc.

Circulation is available at <http://www.circulationaha.org>

DOI: 10.1161/CIRCULATIONAHA.104.524355

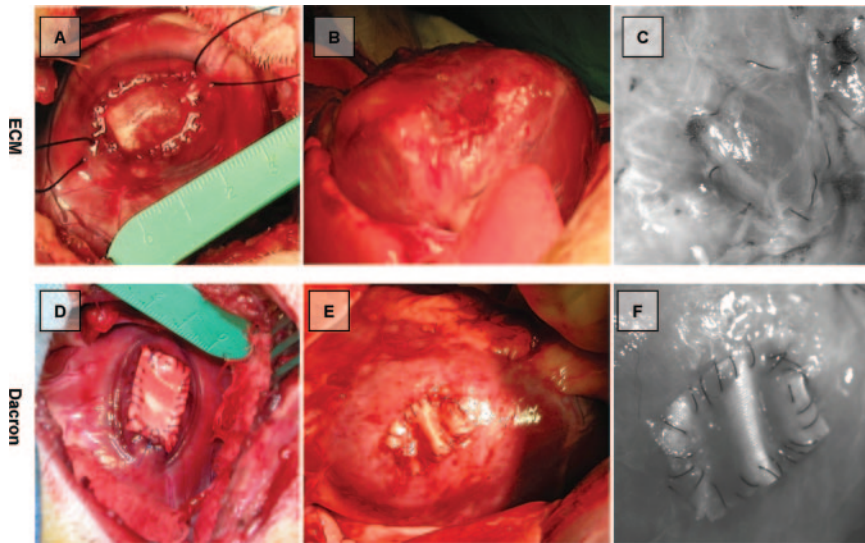


Figure 1. Time series of ECM and Dacron patches. A, ECM at implantation; B, ECM after the 8-week recovery period; C, high-resolution picture of ECM at 8 weeks used in HDM analysis; D, Dacron at implantation; E, Dacron after the 8-week recovery period; and F, high-resolution picture of Dacron used in HDM analysis.

devoid of cells, as a TEMP.¹⁵ Scattered islands of cardiomyocytes were identified on the implant site after 8 weeks.¹⁵

In this study, we hypothesized that ECM would confer mechanical benefit as a result of cardiomyocyte population 8 weeks after myocardial implantation. We tested this hypothesis by implanting ECM in the canine heart, and compared its mechanical function to Dacron, a biologically inactive patch frequently used in surgical restoration of the heart.

Methods

Experimental Animals

All animals received humane care in compliance with the *Principles of Laboratory Animal Care* formulated by the National Society for Medical Research and the *Guide for the Care and Use of Laboratory Animals* prepared by the National Academy of Sciences and published by the National Institutes of Health (NIH Publication No. 85-23, revised 1985). Dogs were divided into 3 groups: Baseline, ECM, and Dacron. The baseline group was subject only to the surgery necessary to establish normal right ventricular (RV) function (n=4). The ECM and Dacron groups each consisted of 5 dogs. Four dogs in each group were subject to both mechanical function evaluation and histological examination. One dog in each group was used solely for histological analysis to confirm that mechanical measurement techniques did not affect histological findings.

Initial Surgery

Adult mongrel dogs weighing 20 to 30 kg were sedated using ketamine, intubated, and placed under general anesthesia using isoflurane. The right chest was entered using a right anteromedial incision over the fifth intercostal space. A pericardial cradle was constructed. Next, a portion of the posterolateral right ventricular free wall was isolated using a Satinsky clamp. A full thickness portion of myocardium approximately 15 by 10 mm was excised. To test the adequacy of the defect, a suture was placed above and below its long axis, and the Satinsky clamp was slowly released. A commensurate portion of ECM (ACell) or Dacron (USCI) was used to repair the defect with a running 5.0 prolene suture (Figure 1A). The clamp was released. Once adequate hemostasis was obtained, the chest was closed in the standard fashion.

Terminal Surgery

Eight weeks later, the animals were returned to the operating room, sedated, intubated, and placed under general anesthesia. A catheter was placed in the femoral artery for hemodynamic monitoring. The

anterior chest wall was removed via bilateral thoracotomy. Adhesions were carefully dissected off the heart to expose the patch and its suture line. A pressure transducer (Millar Instruments) was placed into the RV. Finally, the inferior vena cava (IVC) was isolated, and a length of umbilical tape was placed around it above the level of the diaphragm.

Global Systolic Function

Global function of the RV was studied by determining the preload recruitable stroke work relationship as previously described.¹⁶ Briefly, ultrasonic crystals were secured along 3 axes of the heart: Base to apex, anterior to posterior, and septal to RV free wall. Data were recorded during gradual occlusion of the IVC. At the end of the experiment, the ellipsoidal shell subtraction method was used to calculate RV volume.¹⁷ Volume data were used to create pressure-volume loops for each heartbeat subject to IVC occlusion. Stroke work, defined as the integral of pressure with respect to volume change, was calculated for each heartbeat and plotted against end-diastolic volume, establishing a linear relationship. The slope of this line represents right ventricular contractility, a measure of systolic function independent of heart rate and afterload.¹⁶ This relationship was established using at least 7 consecutive points that decreased stroke work by at least 50%.

Global Diastolic Function

Tau, the time constant for isovolumic relaxation, was calculated based on a method described by Weiss et al¹⁸ and used as a measure of global diastolic function. Right ventricular tau was calculated at 8 weeks for baseline, ECM, and Dacron groups. Data were obtained at the onset of each experiment by recording RV pressure waveforms at a rate of 250 samples per second. At the end of the experiment, RV pressure waveforms during isovolumic relaxation were fit to an exponential decay, allowing for determination of tau.¹⁹

Regional Systolic Function

Regional function was determined by high density mapping (HDM), a technique developed in our laboratory and described in detail elsewhere.²⁰ Briefly, a region of interest (ROI) was selected on the epicardial surface of the heart and covered with speckles. The speckles, composed of silicon carbide particles, created a random high contrast light intensity distribution used to measure epicardial surface deformation. Next, a complimentary metal-oxide semiconductor camera (Photron) was focused on the ROI, and images were taken at 250 frames per second. Using a subpixel extended-phase correlation algorithm,²¹ high-resolution displacement vector maps of epicardial surface deformation during the cardiac cycle were obtained. The vector arrays were used to calculate area change via

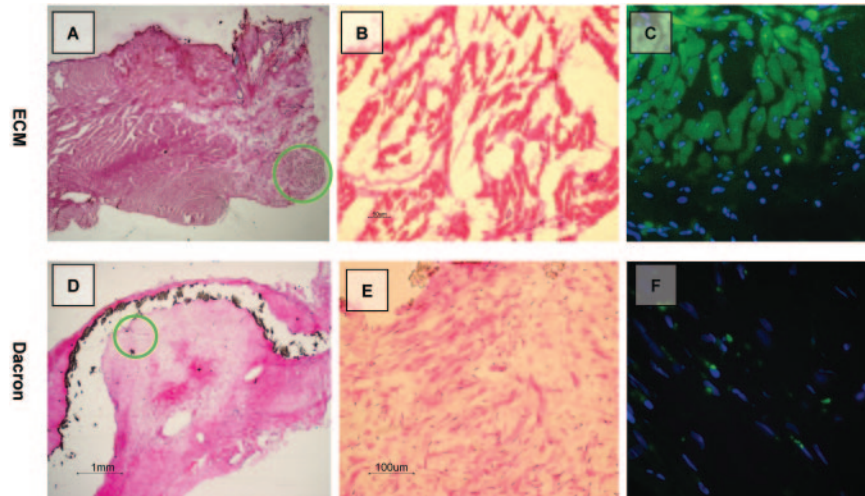


Figure 2. Histological examination of the ECM and Dacron. A, Cross-section of ECM after 8 weeks. Native myocardium is on the left, ECM on right. The green circle represent the regions focused on in B. B, 40 \times magnification of cluster of cells on endocardial surface; C, Alpha sarcomeric actinin staining of some cells found on the ECM patch, suggesting cardiomyocyte population; and D, Cross-section of Dacron after 8 weeks. The green circle represent the regions focused on in panel E. E, 40 \times magnification of the Dacron. Numerous fibroblasts occupy the defect. F, Alpha sarcomeric actinin staining is nonspecific.

Green's theorem between consecutive images and over an entire heartbeat. Systolic area contraction (SAC) was calculated as the difference between the end-diastolic area and the end-systolic area, normalized to the end-diastolic area. To compare hearts with different ROI size, the end-diastolic area was set to 1.

Regional Diastolic Function

The rate and total amount of epicardial shear during diastole were used as measures of diastolic function. Vector maps obtained from HDM were used to calculate epicardial shear through infinitesimal Eulerian strain equations.²² These values were then converted to Lagrangian strain, and the change in shear angle during diastole was computed. Recoil rate, recently shown to be a correlate of tau,²³ was computed by differentiating maximum change in diastolic shear angle with respect to time.

Histology

Specimens of the patch area in all 3 groups were placed in 4% paraformaldehyde and later transferred to 30% sucrose solution. The specimens were then placed in an embedding matrix and sectioned at a thickness of 10 μ m. Measurements of thickness were taken from the middle of each implant. These sections were stained with hematoxylin and eosin and alpha sarcomeric actinin.

Statistical Analysis

All data are expressed as the mean \pm SEM. Statistical analyses between groups were performed by 1-way analysis of variance with a post-hoc Duncan test. Differences were considered significant for probability values less than 0.05.

Results

Mortality and Macroscopic Results

Overall, 17 dogs were included in this study. There were 3 operative deaths, 1 relating to the fragility of the ECM and 2 attributable to arrhythmia. However, mortality dropped to less than 4% in subsequent series with adjustments in protocol, ie, adding a weight-based dosage of lidocaine before placing and releasing the Satinsky clamp.

Mediastinal adhesions were present for both ECM and Dacron groups. On gross appearance, however, there were substantially more adhesions in the Dacron group. Furthermore, a dense layer of connective tissue was evident over the epicardial surface of all Dacron patches. After the removal of overlying connective tissue, the Dacron patch was clearly identifiable (Figure 1D). Aside from a wrinkled appearance,

the patch was unchanged (Figure 1E). Conversely, the ECM implants appeared well integrated with adjacent myocardium (Figure 1B and 1C). A comparable layer of connective tissue was not evident. There was no evidence of aneurysmal dilation in either ECM or Dacron groups.

The average size of the defects for both groups was 16 ± 3 by 10 ± 2 mm. The thickness of ECM at implantation was approximately 150 μ m. Eight weeks later, the average thickness was 2.2 ± 1.1 mm. The average thickness of the Dacron patch at implantation was 250 μ m. Eight weeks later, the average thickness was 2.4 ± 1.0 mm. The average thickness of native myocardium was 5.4 ± 0.8 mm.

Microscopic Results

Histological examination of sections was conducted in both groups (Figure 2). The Dacron group displayed fibroblast proliferation with abundant collagen deposition organized in a dense manner (Figure 2E). The Dacron patch was intact; there was no infiltration by cellular elements. Cardiomyocytes were not evident on the Dacron patch (Figure 2F).

ECM displayed a variety of cell types. Clusters of cardiomyocytes were seen along the endocardial surface (Figure 2B). These cells were organized in a diminishing gradient from the outer border to the center of the implant site, with few cardiomyocytes in the center of the patch. These cells stained positive for alpha sarcomeric actinin (Figure 2C) and were striated and approximately the same size and shape as adjacent native myocytes (Figure 3). The cardiomyocytes on

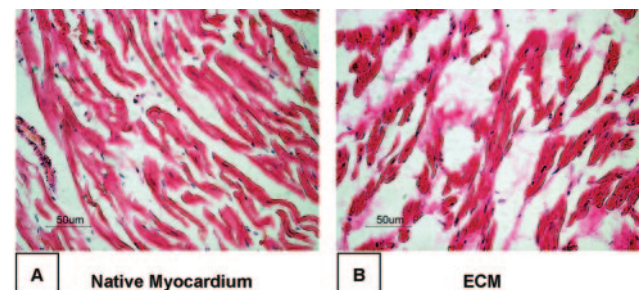


Figure 3. Hematoxylin and eosin staining of (A) native myocardium region compared with (B) cardiomyocytes on the ECM patch under 40 \times magnification.

Summary of Key Parameters and Mechanical Data

	Baseline (n=4)	ECM (n=4)	Dacron (n=4)
ROI, mm by mm	7±1 by 6±2	7±2 by 5±1	10±2 by 7±1
Defect size, mm by mm	...	15±1 by 10±1	18±2 by 11±1
Developed pressure, mm Hg	16±2	21±3	20±3
Heart rate, bpm	89±10	99±5	87±5
Global function			
Contractility, M_w (J/L)	2.0±0.1	1.7±0.2	1.5±0.1
Tau, msec	81±11	86±23	92±17
Regional function			
Systolic area contraction	21.6±1.8	4.1±0.9*	-1.8±1.1*†
Recoil rate, ° sec ⁻¹	-52±8	-44±7	-17±2*†
Diastolic shear, °	5.6±1.3	3.0±0.1	0.0±0.3*

* $P < 0.05$ compared to baseline; † $P < 0.05$ compared to ECM.

ECM were interspersed with adipocytes, a finding which differed from the architecture of native myocardium (Figure 3). Fibroblasts with collagen deposition, scattered macrophages, and leukocytes were also seen. The epicardial aspect of the patch contained numerous blood vessels (Figure 2A).

Global Function

Contractility, used as a measure of global systolic function, was 2.0 J/L in baseline, 1.7 J/L in the ECM, and 1.5 J/L in the Dacron group. There was a 15% and 25% reduction in contractility in ECM and Dacron groups, respectively. The differences were not statistically significant. Global diastolic function, as measured by tau, was similar in all groups. A summary of global function is seen in the Table.

Regional Systolic Function

The average size of the ROI for all groups was 8±1 mm by 6±1 mm. Average SAC in baseline was 21.6±1.8%, whereas the Dacron implants demonstrated essentially no SAC (SAC=-1.8±1.1%). Conversely, the SAC in the 8-week ECM patch region was 4.1±0.9% (Figure 4). This was

significantly lower than baseline ($P < 0.05$), yet significantly higher than Dacron ($P < 0.05$). A summary of regional systolic function is seen in the Table.

Regional Diastolic Function

Regional diastolic function, assessed by spatiotemporal shear deformation, differed between the Dacron and ECM groups. Dacron caused a reversed shear pattern and a lower recoil rate during isovolumic relaxation (Figure 5). The Dacron group had an average diastolic shear of 0.0±0.3°, compared with 5.6±1.3° at baseline ($P < 0.01$). The average diastolic shear of the ECM group was 3.0±0.1°, lower than baseline ($P < 0.05$) and higher than Dacron ($P < 0.05$). The regional recoil rate was -52±8° sec⁻¹, -44±7° sec⁻¹, and -17±2° sec⁻¹ in the baseline, ECM, and Dacron groups, respectively ($P < 0.05$ for both Dacron versus baseline and Dacron versus ECM).

Discussion

The novel finding of our report is that a TEMP derived from ECM contributes to regional function 8 weeks after implantation in the canine heart. In addition, we confirmed cardiomyocyte population of ECM. The etiology of these cells has been under investigation, with possible explanations including the deposition of circulating bone marrow-derived progenitor cells and the fusion of cardiac progenitor cells with host cells.^{24,25} Beltrami et al²⁶ suggested that Lin-C-kit positive stem cells act as key players in myocardial reconstitution. The origin of these cardiomyocytes remains an unanswered question, worthy of future research, but is not the focus of this study.

The regional mechanical benefit in our report is based on a technique that correlates epicardial surface deformation with pressure change. The technique used allows for determination of regional deformation within the boundaries of the patch implantation. Examination of the area changes seen in ECM during the cardiac cycle identifies 2 important findings. First, there is active contraction of the ECM. The pressure-area loop clearly demonstrates regional systolic contraction in the ECM implant. This pattern of deformation can only result

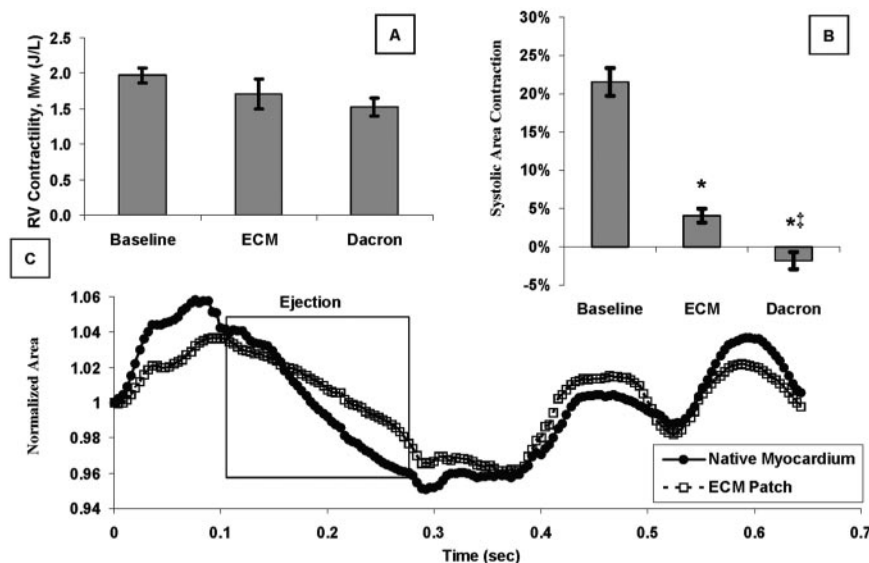


Figure 4. Summary of systolic function parameters. A, Global systolic function, measured by chamber contractility, was similar in all groups. B, Regional systolic area contraction of baseline, ECM, and Dacron were significantly different. * $P < 0.05$ vs baseline; † $P < 0.05$ vs ECM. C, Regional area change vs time of adjacent native myocardium and ECM. Note the synchronous area change between the 2 regions.

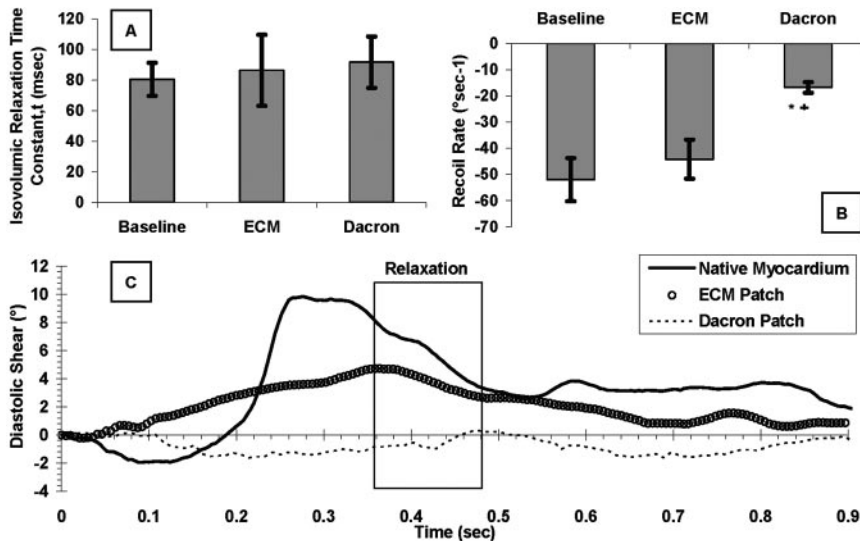


Figure 5. Summary of diastolic function parameters. A, Tau was similar in all groups. B, Recoil rate, used as a measure of regional diastolic function, was significantly reduced in the Dacron group compared with both baseline and ECM groups. C, Spatiotemporal shear distributions from representative animals in baseline, ECM, and Dacron groups, respectively.

from active contraction in the implant region and not passive elastic recoil. Second, this contraction is in synchrony with native myocardium. Although definitive electrophysiological studies were not performed, simultaneously recorded data from ECM and adjacent native myocardium in selected animals clearly demonstrate that the contraction in the implant region is in phase with that of the normal, un-operated on myocardium (Figure 4C). Microscopic evaluation of Dacron patches did not demonstrate the presence of cardiomyocytes nor do the mechanical data indicate that Dacron implantation contributes to regional function. These findings suggest that cardiomyocyte population of ECM is likely responsible for its regional systolic function.

Right ventricular contractility, a measure of global systolic function, was decreased 15% in the ECM group and 25% in the Dacron group when compared with baseline. Although the differences were not statistically significant, power analysis suggests an additional 8 dogs per group would be needed to demonstrate a statistically significant difference. The lack of outright statistical significance may also be related to the small size of the defect created in the RV in relation to its total surface area, a clear limitation of our study. While investigating the relationship of infarct size to cardiac function, Pfeffer et al²⁷ concluded that a significant change in global function would not be evident until at least 20% of the ventricle was compromised. In the present study, approximately 5% of the RV was removed and patched. Additionally, it is unlikely that the single layer of ECM used in our study would withstand left ventricular pressure, thus limiting its applicability in its current state. Increasing the number of ECM layers could be an alternative, but it is unclear if the physiological benefit, ie, cardiomyocyte population, would still be evident.

Grossly, Dacron elicited far greater fibrosis than ECM, correlating with more mediastinal adhesions and epicardial connective tissue deposition. On placement, the Dacron patch was clearly under tension. Surprisingly, 8 weeks after implantation, all Dacron patches had a wrinkled appearance, suggesting the patch was no longer under tension (Figure 1D and 1E). The “wrinkle effect” is likely the result of wound

contraction around Dacron. In sharp contrast, ECM triggered far less fibrosis. The patch was neither wrinkled nor aneurysmal and appeared to share the same surface tension as adjacent native myocardium. Finally, after removal of adhesions, it was difficult to grossly distinguish ECM from native myocardium (Figure 1C). The quantitative and qualitative differences between ECM and Dacron could be explained by an inherent ability of ECM to house cellular elements that facilitate remodeling.

Our results examining diastolic function were similar to those we obtained for systolic function. Tau, the time constant for isovolumic relaxation, was similar in all 3 groups. The differences in regional diastolic function between ECM and Dacron are likely the result of the cells found on the implant region and the compliance mismatch between native myocardium and the patch. The modulus of elasticity of Dacron is at least 4 orders of magnitude greater than healthy myocardium, ie, Dacron is stiffer than myocardium. Thus, the use of Dacron as a myocardial patch may have a “tethering effect” that would reduce the mechanical function of surrounding myocardium. Furthermore, the cellular response to Dacron was primarily diffuse fibroblast proliferation, an observation also seen with remodeling after myocardial infarction. In contrast, ECM stimulated less fibrosis and was populated by different cell types, including cardiomyocytes. Atkins et al²⁸ have shown that the reduction of infarct stiffness via cell transplantation leads to increased diastolic function. Similarly, Quarterman et al²⁹ created a detailed finite element model to show that cell transplantation alone will result in changes in compliance that result in mechanical benefit.

The potential clinical applications of ECM as a scaffold are many and would have a powerful impact on the management of cardiac disease. These would include instances in which Dacron is presently used as a myocardial patch: repair of ventricular aneurysms, repair of congenital heart defects, and most recently, surgical restoration of a dyskinetic or akinetic ventricle. By its contribution to regional systolic function, ECM provides true restoration of the ventricle rather than nonfunctional substitution of defective tissue, as is the case

with Dacron. Furthermore, it already has Food and Drug Administration approval for several indications, potentially facilitating its use in humans as a TEMP.

Acknowledgments

This study was supported by grants from the National Institute of Health HL20558 (Dr Cohen), HL28958 (Dr Cohen), HL67101 (Dr Cohen), and EB000261 (Dr Badylak), and the New York State Office of Science, Technology, and Academic Research (Dr Gaudette). We greatly appreciated the effort of Peter V. Kochupura, MD, for his vigorous review of this manuscript.

References

- Jessup M, Brozena S. Heart failure. *N Engl J Med*. 2003;348:2007–2018.
- Patel J, Kobashigawa JA. Cardiac transplantation: the alternate list and expansion of the donor pool. *Curr Opin Cardiol*. 2004;19:162–165.
- American Heart Association. *2004 Heart and Stroke Statistical Update*. American Heart Association: Dallas Tex; 2004.
- Loebe M, Soltero E, Tohan V, Lafuente JA, Noon GP. New surgical therapies for heart failure. *Curr Opin Cardiol*. 2003;18:194–198.
- Coolley DA, Frazier OH, Duncan JM, Reul GJ, Krajcer Z. Intracavitary repair of ventricular aneurysm and regional dyskinesia. *Ann Surg*. 1992; 215:417–423.
- Dor V. The endoventricular circular patch plasty (“Dor procedure”) in ischemic akinetic dilated ventricles. *Heart Fail Rev*. 2001;6:187–193.
- Buckberg GD. Basic science review: the helix and the heart. *J Thorac Cardiovasc Surg*. 2002;124:863–883.
- Buckberg GD. Congestive heart failure: treat the disease, not the symptom: return to normalcy. *J Thorac Cardiovasc Surg*. 2001;121: 628–637.
- Jatene AD. Left ventricular aneurysmectomy: resection or reconstruction. *J Thorac Cardiovasc Surg*. 1985;89:321–331.
- Di Donato M, Sabatier M, Dor V, Gensini GF, Toso A, Maioli M, Stanley AW, Athanasuleas C, Buckberg G. Effects of the Dor procedure on left ventricular dimension and shape and geometric correlates of mitral regurgitation one year after surgery. *J Thorac Cardiovasc Surg*. 2001;121: 91–96.
- Krupnick AS, Kreisel D, Riha M, Balsara KR, Rosengard BR. Myocardial tissue engineering and regeneration as a therapeutic alternative to transplantation. *Curr Top Microbiol Immunol*. 2004;280:139–164.
- Zimmermann WH, Didie M, Wasmeier GH, Nixdorff U, Hess A, Melnychenko I, Boy O, Neuhuber WL, Weyand M, Eschenhagen T. Cardiac grafting of engineered heart tissue in syngenic rats. *Circulation*. 2002;106(suppl 1):I-151-I157.
- Matsubayashi K, Fedak PW, Mickle DA, Weisel RD, Ozawa T, Li RK. Improved left ventricular aneurysm repair with bioengineered vascular smooth muscle grafts. *Circulation*. 2003;108(suppl II):II-219-III-225.
- Kofidis T, Akhyari P, Boublik J, Theodorou P, Martin U, Ruhparwar A, Fischer S, Eschenhagen T, Kubis HP, Kraft T, Leyh R, Haverich A. In vitro engineering of heart muscle: artificial myocardial tissue. *J Thorac Cardiovasc Surg*. 2002;124:63–69.
- Badylak S, Obermiller J, Geddes L, Matheny R. Extracellular matrix for myocardial repair. *Heart Surg Forum*. 2003;6:E20–E26.
- Glower DD, Spratt JA, Snow ND, Kabas JS, Davis JW, Olsen CO, Tyson GS, Sabiston DC Jr, Rankin JS. Linearity of the Frank-Starling relationship in the intact heart: the concept of preload recruitable stroke work. *Circulation*. 1985;71:994–1009.
- Feneley MP, Elbeery JR, Gaynor JW, Gall SA Jr, Davis JW, Rankin JS. Ellipsoidal shell subtraction model of right ventricular volume: comparison with regional free wall dimensions as indexes of right ventricular function. *Circ Res*. 1990;67:1427–1436.
- Weiss JL, Frederiksen JW, Weisfeldt ML. Hemodynamic determinants of the time-course of fall in canine left ventricular pressure. *J Clin Invest*. 1976;58:751–760.
- Pasipoularides AD, Shu M, Shah A, Glower DD. Right ventricular diastolic relaxation in conscious dog models of pressure overload, volume overload, and ischemia. *J Thorac Cardiovasc Surg*. 2002;124:964–972.
- Gaudette GR, Todaro J, Krukenkamp IB, Chiang FP. Computer aided speckle interferometry: a technique for measuring deformation of the surface of the heart. *Ann Biomed Eng*. 2001;29:775–780.
- Foroosh H, Zerubia JB, Berthod M. Extension of phase correlation to subpixel registration. *IEEE Trans Image Proces*. 2002;11:188–200.
- Malvern LE. *Introduction to the Mechanics of a Continuous Medium*. Upper Saddle River, NJ: Prentice-Hall Inc; 1969.
- Dong SJ, Hees PS, Siu CO, Weiss JL, Shapiro EP. MRI assessment of LV relaxation by untwisting rate: a new isovolumic phase measure of tau. *Am J Physiol Heart Circ Physiol*. 2001;281:H2002–H2009.
- Deb A, Wang S, Skelding KA, Miller D, Simper D, Caplice NM. Bone marrow-derived cardiomyocytes are present in adult human heart: a study of gender-mismatched bone marrow transplantation patients. *Circulation*. 2003;107:1247–1249.
- Oh H, Bradfute SB, Gallardo TD, Nakamura T, Gausson V, Mishina Y, Pocius J, Michael LH, Behringer RR, Garry DJ, Entman ML, Schneider MD. Cardiac progenitor cells from adult myocardium: homing, differentiation, and fusion after infarction. *Proc Natl Acad Sci U S A*. 2003;100: 12313–12318.
- Beltrami AP, Barlucchi L, Torella D, Baker M, Limana F, Chimenti S, Kasahara H, Rota M, Musso E, Urbaneck K, Leri A, Kajstura J, Nadal-Ginard B, Anversa P. Adult cardiac stem cells are multipotent and support myocardial regeneration. *Cell*. 2003;114:763–776.
- Pfeffer MA, Pfeffer JM, Fishbein MC, Fletcher PJ, Spadaro J, Kloner RA, Braunwald E. Myocardial infarct size and ventricular function in rats. *Circ Res*. 1979;44:503–512.
- Atkins BZ, Huelman MT, Meuchel J, Hutcheson KA, Glower DD, Taylor DA. Cellular cardiomyoplasty improves diastolic properties of injured heart. *J Surg Res*. 1999;85:234–242.
- Quarterman RL, Moonly S, Wallace AW, Guccione J, Ratcliffe MB. A finite element model of left ventricular cellular transplantation in dilated cardiomyopathy. *ASAIO J*. 2002;48:508–513.